ORIGINAL ARTICLE

Renal stone detection using a low kilo-voltage paediatric CT protocol – a porcine phantom study

Bo Mussmann, MSc, PhD,[1,2,3] iD Maryann Hardy, PhD,[2,4] Helene Jung, MD, PhD,[5,6] Ming Ding, MD, PhD,[7,8] Palle J. Osther, MD, PhD,[5,6] Maja Lynge Fransen, MD,[1] Pernille Wied Greisen, MD,[1] & Ole Graumann, MD, PhD[1,2]

[1]Department of Radiology, Odense University Hospital, Odense, Denmark
[2]Research and Innovation Unit of Radiology, University of Southern Denmark, Odense, Denmark
[3]Faculty of Health Sciences, Oslo Metropolitan University, Oslo, Norway
[4]Faculty of Health Studies, University of Bradford, Bradford, UK
[5]Urological Research Center, Department of Urology, Lillebaelt Hospital, Vejle, Denmark
[6]Department of Regional Health Research, University of Southern Denmark, Odense, Denmark
[7]Department of Orthopaedic surgery and traumatology, Odense University Hospital, Odense, Denmark
[8]Department of Clinical Research, University of Southern Denmark, Odense, Denmark

Abstract

Introduction: Reducing tube voltage is an effective dose saving method in computed tomography (CT) assuming tube current is not concurrently increased. Recent innovations in scanner technology now enable CT tube voltage reduction to 70 kV thereby increasing opportunities for dose reduction in paediatric patients, but it is unclear if the increased image noise associated with 70 kV impacts on ability to visualise renal stones accurately. The purpose was to assess detectability of nephrolithiasis using a bespoke paediatric phantom and low kV, non-contrast CT and to assess inter-observer agreement. **Methods:** Forty-two renal stones of different size and chemical composition were inserted into porcine kidneys and positioned in a bespoke, water-filled phantom mimicking a 9-year-old child weighing approximately 33kg. The phantom was scanned using 120 and 70 kV CT protocols, and the detectability of the stones was assessed by three radiologists. Absolute agreement and Fleiss' kappa regarding detectability were assessed. **Results:** The mean diameter of renal stones as measured physically was 4.24 mm ranging from 1 to 11 mm. Four stones were missed by at least one observer. One observer had a sensitivity of 93 and 95% at 70 and 120 kV, respectively, while the sensitivity for observers 2 and 3 was 98% at both kV levels. Specificity was 100% across readers and kV levels. Absolute agreement between the readers at 70 kV was 92% (kappa = 0.86) and 98% (kappa = 0.96) at 120 kV indicating a strong agreement at both kV levels. **Conclusions:** The results suggest that lowering the kV does not affect the detection rate of renal stones and may be a useful dose reduction strategy for assessment of nephrolithiasis in children.

Introduction

Over the past decades, the incidence of paediatric and adolescent renal stones has increased globally resulting in a greater risk of renal stone-related morbidity and recurrences in adulthood.[1–3] This increasing incidence is clearly reflected in the number of paediatric stone treatments undertaken locally in the Region of Southern Denmark, with 12 surgeries recorded in children <18 years of age in 2014 and 89 in 2019 (extract from Hospital records). Depending on the underlying cause of stone formation, paediatric patients will have to be monitored for recurrence over several years. Typically, this is undertaken using ultrasound, with non-contrast computed tomography (NCCT) being used when ultrasound is inconclusive[4,5] or when surgical

intervention is required.[6,7] As the paediatric population are at higher risk of radiation-induced cancer as a consequence of physiology and longer expected life span,[8] it is essential that clinical practice adopts dose optimisation and dose reduction strategies to limit risk. New CT technology provides the option of using low kV dose reduction protocols which will benefit paediatric patients. However, before implementation, it is vital to ensure that the benefits of low kV protocols are not offset by reduced diagnostic accuracy.

Reducing tube voltage is an effective method of dose reduction[9,10] if the tube current is not concurrently increased to compensate for the reduction in transferred image-forming photons. Using a lower kV will result in an increase in noise but also image contrast as a consequence of an increased proportion of photoelectric effect and relative reduction in Compton scatter. Furthermore, in small children, the mA often reaches or approaches the lower mA limit at 120 kV, which may restrain the utility of the automatic exposure control. As a result, some studies have explored reducing voltage from 120 kV (common standard) to 100 or 80 kV.[11,12] Recent innovations in scanner technology include reducing tube voltage to 70 kV[13] thereby increasing opportunities for further dose reduction in paediatric patients, but it is unclear if the increased image noise associated with further decrease in kV impacts ability to accurately visualise renal stones. The purpose of this experimental porcine ex-vivo study was to assess the detectability of nephrolithiasis using low kV NCCT and the effect of low kV on accurate stone diameter measurement. The hypothesis was that renal stones could be detected and measured using NCCT with the same confidence using 70 kV compared to a 120 kV protocol.

Methods

The work was considered by the appropriate Panel of the Committee for Ethics in Research at the University of Bradford and it was concluded that ethical approval was not needed since the project did not involve human participants and the previously removed renal stones used in the study were deemed non-biological.

The 42 renal stones used in this study were borrowed from the Department of Urology, Lillebaelt Hospital, Vejle, Denmark. These stones had been previously removed from 20 patients during surgery (10 female, nine male, one unknown; mean age 59 years (range 40–74). The chemical composition of the stones was determined using Fourier transform infrared spectroscopy which classified the stones as brushite ($n = 6$); calcium–phosphate/struvite ($n = 1$); calcium oxalate dihydrate (COD) ($n = 5$); calcium oxalate monohydrate (COM)

Figure 1. Water-filled phantom with four porcine kidneys attached to a plastic ledge. The mean circumference for an average 9 years old boy/girl: 63.6cm/62.6cm respectively while the phantom circumference is 63cm.

($n = 18$); COM/calcium–phosphate ($n = 5$); cystine ($n = 5$); uric acid ($n = 1$); and carbonite–apatite ($n = 1$). All of these stone compositions are known to occur in a paediatric population.[14] The widest diameter of the stones was determined using a millimetre measured ruler with the exact diameter of seven stones being additionally determined by micro-CT (Scanco VivaCT40, Scanco Medical, Brüttisellen, Switzerland) to assist in assuring visual measurement accuracy.

A bespoke, water-filled, cylindrical Perspex phantom containing four porcine kidneys was used for the experiment (Fig. 1). The phantom diameter was 200 mm mimicking a 9-year-old child and corresponds to a young adolescent[15] weighing approximately 33 kg.[16] This size was chosen as urolithiasis in children <9 years is less frequent[17] and low kV imaging is most applicable in young individuals who are more sensitive. Similar to previous studies[18,19] a coronal incision was made in each kidney to allow for positioning of kidney stones in the calyces. One, two or no stones were inserted into each kidney before imaging was performed. The decision on number of stones in each kidney was made in an arbitrary attempt to obtain variation and to mimic clinical reality.

Imaging procedure

All scans were performed using a GE Revolution CT scanner (GE Healthcare, Waukesha, WI, USA) and a low-dose 120 kV clinical protocol and a 70 kV protocol. The noise index (i.e. the vendor-specific image quality metric) of the 70 kV protocol was increased to avoid

Table 1. Acquisition parameters for the scan protocols.[*]

Parameter	Standard protocol	Low kV protocol
Tube voltage	120 kV	70 kV
Tube current modulation range	20–740 mA	10–740 mA
Noise Index	28	38
$CTDI_{vol}$	1.33 mGy	0.49 mGy
Scan Field of View	50 cm	50 cm
Scan range	51 cm	51 cm
Scan time	0.5 s	0.5 s
Pitch	0.5	0.5
Collimation	128 × 0.625 mm	128 × 0.625 mm
Kernel	Standard	Standard
ASIR-V[*]	40%	40%

ASIR-V, Adaptive Statistical Iterative Reconstruction.

compensatory tube current increase by the automatic exposure control. The scan parameters are detailed in Table 1. The effective radiation dose in millisievert (mSv) was calculated using dose–length product (DLP) multiplied by the abdomen specific conversion factor $k = 0.015$.[20,21]

Image analysis

The images were independently evaluated by three radiologists with 14 (R1), 11 (R2) and 7 (R3) years of experience within radiology as specialists in abdominal pathology. One radiologist (R1) was asked to record the position and widest diameter of all visible calculi using Centricity PACS RA1000 Workstation (GE Healthcare, Waukesha, IL, US) equipped with 21.3" CCL358i2/F diagnostic monitors (JVCKenwood Corp., Yokohama, Japan) with 3 megapixel resolution. These stone diameter measurements as determined using CT were compared against the physical diameter measurements for similarity and agreement. Two additional radiologists were asked to record the presence and position of stones for inter-observer analysis regarding detectability. The radiologists were blinded to the number, type and size of the calculi and by default; the images were presented for evaluation using a bone window although the radiologists were able to manipulate post-processing parameters (e.g. window-width, window-level, magnification). Reformatted slice thickness was 2.5 mm in the transverse plane and 5 mm in the coronal and sagittal planes (Fig. 2). The order of image presentation was consistent with radiologists first assessing images acquired at 70 kV and then those acquired at 120 kV. A minimum time of 4 weeks elapsed between reviewing the 70 kV and 120 kV image series to eliminate recall bias. The attenuation and standard

deviation were measured by observer 1 using ROIs positioned in a homogeneous section of the kidney parenchyma (~70 mm^2) and in the centre of each detected stone, and contrast-to-noise ratio (CNR) was calculated using the formula below.

$$CNR = \frac{\left| HU_{Stone} - HU_{Kidney} \right|}{SD_{Kidney}}$$

Statistical analysis

Continuous variables were summarised using descriptive statistics, and normality was assessed using the Shapiro–Wilk test. Differences between continuous, normally distributed variables were analysed using parametric tests. Nominal variables were summarised by proportions, and differences were assessed using Wilcoxon signed rank test. Inter-observer agreement was determined using per cent absolute agreement and the Fleiss Kappa statistic.[22] P-values <0.05 were considered statistically significant. All analyses were performed using STATA/IC 16 (StataCorp. LP, College Station, TX, USA).

Results

In total, 42 stones were inserted into the porcine kidneys.

Stone size and attenuation

The mean diameter of the stones as measured physically was 4.24 mm ranging from 1 to 11 mm. The mean diameter as measured by CT at 70 kV was 3.97 mm (range 2–11, $P = 0.0007$), and similarly, at 120 kV, the mean diameter was 3.97 mm (range 2–11, $P = 0.0026$). The difference between physical and CT-based measurements was statistically significant at both 70 kV and 120 kV although not considered to be clinically relevant. For the seven stones with additional micro-CT measurement, no statistically or clinically significant difference was found when compared with physical diameter (mean difference 0.004 mm, SD = 0.22, $P = 0.9652$). The attenuation of the stones at 120 kV ranged from 69 HU (COM/ calcium–phosphate stone) to 1272 HU (COM stone) with large overlap between all stone types. At 70 kV, the minimum and maximum attenuation was 82 and 1844 HU, respectively (Table 2).

Detection

In total, twelve scans were performed, each with images of four kidneys resulting in 48 cases. In 32 cases, one stone was inserted; in five cases, two stones inserted; and in 11 cases, no stones were inserted. Four of the stones
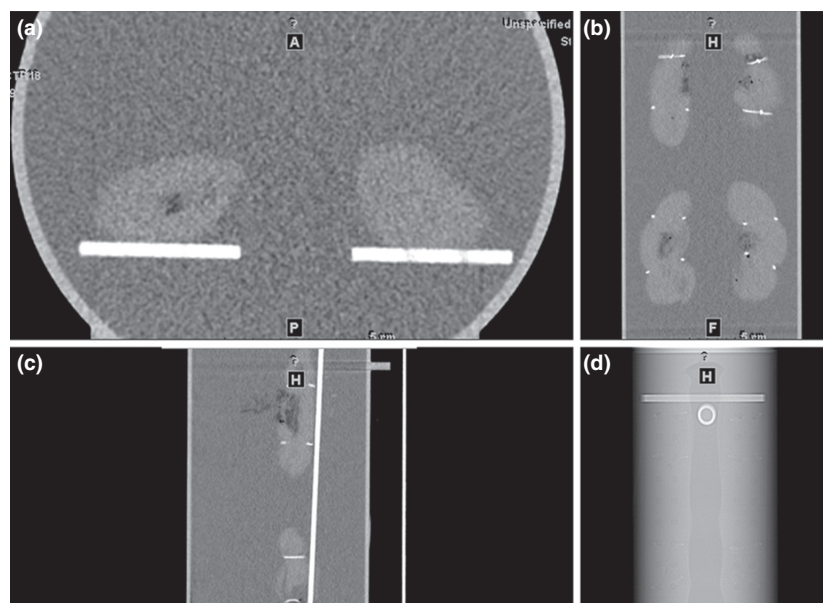
Figure 2. Image reconstructions as presented to the observers. (A) 2.5 mm axial. (B) 5 mm coronal. (C) 5 mm sagittal. The white artefacts in the kidney surface seen in (A) and (B) are elastic bands keeping the kidneys in place. (D) Scout view illustrating the bespoke phantom.

Table 2. Composition and attenuation in Hounsfield Units (HU) and contrast-to-noise ratio (CNR) of detected stones at 70 and 120 kV. Only stones detected were included; $N = 39$.

Composition	N	Mean physical diameter (SD)	Mean attenuation 70 kV (SD; range)	Mean attenuation 120 kV (SD, range)	Mean CNR 70 kV (SD)	Mean CNR 120 kV (SD)
Brushite	6	5.5 (2.7)	847 HU (456; 179-1493)	683 HU (339; 120-1059)	42.0 (25.2)	35.9 (19.3)
CAP-Struvite	1	11.0 (na)	766 HU (na)	575 HU (na)	32.5 (na)	26.2 (na)
COD	5	3.4 (1.1)	476 HU (412; 209-1199)	388 HU (283; 220-879)	20.9 (17.7)	18.4 (15.0)
COM	16	4.25 (2.0)	692 HU (532; 120-1844)	548 HU (379; 93-1272)	29.6 (24.1)	27.1 (20.4)
COM/CAP	5	3.4 (0.8)	355 HU (219; 82-560)	363 HU (179; 69-526)	20.7 (13.6)	17.9 (10.4)
Cystine	4	4.5 (1.3)	510 HU (303; 140-882)	472 HU (176; 255-686)	20.7 (13.6)	23.9 (9.0)
Uric Acid	1	5.0 (na)	298 HU (na)	295 HU (na)	11.2 (na)	13.3 (na)
Carbonite–apatite	1	2.5 (na)	191 HU (na)	254 HU (na)	6.3 (na)	11.4 (na)
Total	39		–	–	26.4 (21.4)	25.1 (17.2)

CAP, calcium–phosphate; COD, calcium oxalate dehydrate; COM, calcium oxalate monohydrate; na, not applicable.

were missed by at least one observer (1 cystine and 3 COM). The size, composition and distribution of missed stones for each observer and kV are shown in Table 3. For observer 1, the sensitivity was 93% at 70 kV and 95% at 120 kV while the sensitivity for observer 2 and 3 was 98% at both kV levels. No false-positive cases occurred, and therefore, specificity was 100% across all readers and kV levels. Absolute agreement between the readers at 70 kV was 92% (95% CI 0.90–1.00), $k = 0.86$. At 120 kV, the agreement was 98% (95% CI 0.96–1.00), $k = 0.96$ indicating strong agreement at both kV levels.

Table 3. Overview of the composition and diameter of the four stones missed by at least one observer (R1, R2 or R3) at 70 or 120 kV.

Composition of missed stones	Diameter (mm)	Observer 70 kV	Observer 120 kV
Cystine	1.0	R1	R1
COM	1.0	R1, R3	R1, R2, R3
COM	3.0	R1	
COM	2.5	R2	

COM, calcium oxalate monohydrate.

Radiation dose and image quality

The mA range in the acquired scans was 19–20 mA at 120 kV (i.e. the lowest possible mA) and 32 to 39 mA at 70 kV. Using the 120 kV protocol, mean DLP was 68.0 mGy*cm (SD = 0.96) whereas using the 70 kV protocol, mean DLP was 25.2 mGy*cm (SD = 0.72). The effective dose was 1.02 mSv with 120 kV CT and 0.37 mSv with 70 kV representing a dose reduction of 63.7% ($P < 0.0001$). Mean CNR difference between 120 and 70 kV was −1.37 (SD 6.6) ($P = 0.2026$, 95%CI-3.5 to 0.77).

Discussion

In this experimental study, we set out to evaluate possible practice changes prior to human evaluation and implementation thereby reducing experimental risk to paediatric patients. To reflect clinical practice, we included stones with a relatively broad range of chemical compositions, attenuations and sizes, and performed scans with and without inserted stones.

Both CT protocols reflected low dose compared to the European diagnostic reference level (DRL) (DLP = 210 mGy*cm for abdominal CT in children weighing 30–50 kg[15]), but the dose received at 70 kV was significantly lower. Even though the European DRL is for routine abdominal CT requiring higher dose than CT aimed at stone detection, the current study obtained a dose eightfold below that of the DRL despite the scan length being almost doubled compared to that of the DRL (51 vs. 29 cm).

Two observers each missed one relatively large stone (2.5 and 3.0 mm COM) on the low kV protocol images. The false-negative interpretations probably reflect the impact of human factors on image reading and the clinical reality that obvious findings are sometimes overlooked. This error might have also resulted from the clinically unfamiliar presentation of four kidneys on one scan. The same stones were detected at 120 kV while a 1.0 mm COM stone that was detected by one observer at 70 kV was missed by that observer at 120 kV. As COM and cystine stones are highly attenuating at both kV levels as reflected in the CNRs (Table 2) and therefore easily distinguishable from soft tissue, we believe the difference in detection to be caused by random variation and not by kV alteration. As illustrated in Figure 3 the low-kV image quality is inferior to 120 kV regarding noise, but the detectability of renal stones was similar between the kV levels suggesting that dose reduced 70 kV NCCT may be feasible for follow-up purposes regardless of stone composition.

The results of this experimental study concur with the findings of previous studies[12,19] but the results were obtained at even lower kV values and with an effective dose <1 mSv. All 120 kV scans were acquired with the lowest possible mA, and thus, no further dose reduction was possible through mA reduction via automatic exposure control at 120 kV. However, the study has some limitations. The experiment was undertaken using a phantom to simulate the paediatric body. Currently, paediatric abdominal phantoms available for purchase are unsuitable due to inability to insert calculi in the upper urinary tract. The bespoke phantom addressed this concern but the phantom size could not be altered, and therefore, the results do not reflect clinical reality in terms of variation in body size and habitus. As a result, the clinical utility of 70 kV imaging in larger patients approaching adulthood is not addressed in the current study. Despite porcine kidneys being marginally longer
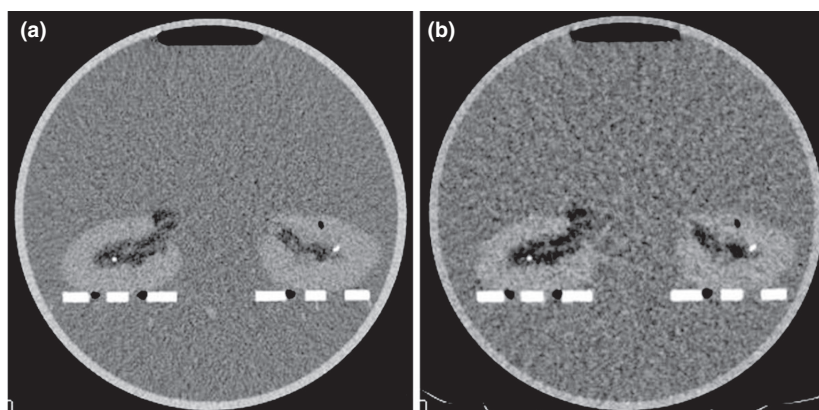

Figure 3. CT Scans acquired using 120 kV (A) and 70 kV (B) showing porcine kidneys with cystine stones immersed in a water phantom. The stones are visible in both kidneys at both kV levels despite noise being more prominent in the low-kV scan.

than those of a 9-year-old child (~12 cm vs. ~10 cm depending on the height of the child[23]), porcine specimens have comparable anatomical and radiographic properties to the human body[24] in terms of attenuation and number of calyces. The cylindrical shape and relatively small phantom diameter must be taken into consideration as the paediatric body is slightly elliptical, and therefore, in a patient, the automatic exposure control would expectedly increase the tube current laterally.

Conclusion

While findings of this study must be confirmed in a prospective clinical study before implementation, and despite the aforementioned limitations, the study results clearly suggest that CT radiation dose can be reduced by lowering the kV value without affecting the detection rate of renal stones. These findings therefore present an opportunity for increasing patient safety in the paediatric population monitored for urolithiasis using NCCT, and the potential reduction in risk of radiation induced cancer in children.

Acknowledgements

References

1. Bonzo JR, Tasian GE. The emergence of kidney stone disease during childhood-impact on adults. *Curr Urol Rep* 2017; **18**: 44.

2. Ristau BT, Dudley AG, Casella DP, et al. Tracking of radiation exposure in pediatric stone patients: the time is now. *J Pediatr Urol* 2015; **11**: 339.e1–5.

3. Clayton DB, Pope JC. The increasing pediatric stone disease problem. *Ther Adv Urol* 2011; **3**: 3–12.

4. Palmer JS, Donaher ER, O'Riordan MA, Dell KM. Diagnosis of pediatric urolithiasis: role of ultrasound and computerized tomography. *J Urol* 2005; **174**(4 Pt 1): 1413–6.

5. Strohmaier WL. Imaging in pediatric urolithiasis-what's the best choice? *Transl Pediatr* 2015; **4**: 36–40.

6. Gedik A, Tutus A, Kayan D, Yilmaz Y, Bircan K. Percutaneous nephrolithotomy in pediatric patients: is computerized tomography a must? *Urol Res* 2011; **39**: 45–9.

7. Jung H, Andonian S, Assimos D, et al. Urolithiasis: evaluation, dietary factors, and medical management: an update of the 2014 SIU-ICUD international consultation on stone disease. *World J Urol* 2017; **35**: 1331–40.

8. Brenner D, Elliston C, Hall E, Berdon W. Estimated risks of radiation-induced fatal cancer from pediatric CT. *AJR Am J Roentgenol* 2001; **176**: 289–96.

9. Shimonobo T, Funama Y, Utsunomiya D, et al. Low-tube-voltage selection for non-contrast-enhanced CT: comparison of the radiation dose in pediatric and adult phantoms. *Phys Med* 2016; **32**: 197–201.

10. Berlin SC, Weinert DM, Vasavada PS, et al. Successful dose reduction using reduced tube voltage with hybrid iterative reconstruction in pediatric abdominal CT. *AJR Am J Roentgenol* 2015; **205**: 392–9.

11. Choi SY, Ahn SH, Choi JD, et al. Determination of optimal imaging settings for urolithiasis CT using filtered back projection (FBP), statistical iterative reconstruction (IR) and knowledge-based iterative model reconstruction (IMR): a physical human phantom study. *Br J Radiol* 2016; **89**: 20150527.

12. Sade R, Ogul H, Eren S, Levent A, Kantarci M. Comparison of ultrasonography and low-dose computed tomography for the diagnosis of pediatric urolithiasis in the Emergency Department. *Eurasian J Med* 2017; **49**: 128–31.

13. Runge VM, Marquez H, Andreisek G, Valavanis A, Alkadhi H. Recent technological advances in computed tomography and the clinical impact therein. *Invest Radiol* 2015; **50**: 119–27.

14. Chu DI, Tasian GE, Copelovitch L. Pediatric kidney stones – avoidance and treatment. *Curr Treat Options Pediatr* 2016; **2**: 104–11.

15. Damilakis J, Järvinen H, Hierath M, et al. European Guidelines on Diagnostic Reference Levels for Paediatric Imaging. European Commission, Luxembourg, 2018. Report No.: 978–92-79-89876-1.

16. Fredriksen PM, Skår A, Mamen A. Waist circumference in 6–12-year-old children: the Health Oriented Pedagogical Project (HOPP). *Scand J Public Health* 2018; **46** (21_suppl): 12–20.

17. Shoag J, Tasian GE, Goldfarb DS, Eisner BH. The new epidemiology of nephrolithiasis. *Adv Chronic Kidney Dis* 2015; **22**: 273–8.

18. Mussmann B, Hardy M, Jung H, Ding M, Osther PJ, Graumann O. Can dual energy CT with fast kV-switching determine renal stone composition accurately? *Acad Radiol* 2021; **28**: 333–8.

19. Talso M, Emiliani E, Froio S, et al. Low-dose CT scan in stone detection for stone treatment follow-up: is there a relation between stone composition and radiation delivery? Study on a porcine-kidney model. *Minerva Urol Nefrol* 2019; **71**: 63–71.

20. Huda W, Ogden KM, Khorasani MR. Converting dose-length product to effective dose at CT. *Radiology* 2008; **248**: 995–1003.

21. Dougeni E, Faulkner K, Panayiotakis G. A review of patient dose and optimisation methods in adult and paediatric CT scanning. *Eur J Radiol* 2012; **81**: e665–83.

22. Fleiss JL. Measuring nominal scale agreement among many raters. *Psychol Bull* 1971; **76**: 378–82.

23. Hodson CJ, Drewe JA, Karn MN, King A. Renal size in normal children: a radiographic study during life. *Arch Dis Child* 1962; **37**: 616–22.

24. Zarb F, McEntee MF, Rainford L. CT radiation dose and image quality optimization using a porcine model. *Radiol Technol* 2013; **85**: 127–36.